ANALYSIS OF DDS-CONTROLLED LOUDSPEAKER ARRAYS BY 'NEAR FIELD ACOUSTIC HOLOGRAPHY'

E.W. Start Duran Audio BV, Zaltbommel, The Netherlands
G.W.J. van Beuningen Duran Audio BV, Zaltbommel, The Netherlands

ABSTRACT

With the recent introduction of 'Digital Directivity Synthesis' (DDS) for loudspeaker arrays, the *synthesis* of optimized, complex-shaped radiation patterns has become possible. Using special simulation software the array response can be predicted in the far as well as in the near field.
This paper describes the *analysis* and verification of DDS-controlled sound fields by measurements. Since anechoic measurements on large arrays are often practically impossible and moreover, not always meaningful, an adapted 'Near field Acoustic Holography' technique is used to measure the predicted array response. By taking impulse responses along a line parallel to the line array, at a short distance, the emitted wave field can be fully characterized in the plane through the array and the measurement (or hologram) line. Next, the measured wave field can be extrapolated to any other position in this vertical plane (within the aperture of the hologram) using a so-called '2½D' wave field extrapolation operator. The advantages of this method will be discussed and also simulated and measured data will be compared.

1 INTRODUCTION

Recently, a new array control concept was introduced [1,2], called 'Digital Directivity Synthesis (DDS)'. Using DDS, which is based on a 'constrained least squares' optimization scheme, any desired 3D array response can be synthesized. Starting from a pre-defined array set-up and desired SPL distribution at the boundaries (including the audience area) of a (fictive) hall, the optimum driving filters for the array elements can be calculated.
Until now a detailed comparison between simulated and measured responses of DDS-controlled arrays has never been made. The reasons for this are two-fold. First, anechoic *far* field directivity measurements are practically impossible and, moreover, since the majority of the listeners is in the *near* field, not always meaningful. Secondly, on-site direct sound measurements in the audience plane and at the boundaries of the hall are troublesome and inaccurate because of the lack of sufficient temporal discrimination between the direct sound and the first reflections. Therefore, an adapted 'Near field Acoustic Holography' technique will be introduced to measure the predicted array response.

2 Near Field Acoustic Holography

In this section the basic principles of 'Near Field Acoustic Holography' and wave field extrapolation will be explained. Also, an adapted, more efficient version of the full 3D extrapolation operator, the so-called '2½D' wave field extrapolation operator, will be introduced.

2.1 Principles

Acoustic Holography is a technique which allows the prediction of any acoustic quantity, intensity, pressure or particle velocity, at a different spatial location than the measured hologram position. The hologram is the plane in which the original measurements are taken and from which the wave field extrapolation (or propagation) is started. Propagation away from the source is generally referred to as forward wave field extrapolation, while propagation towards the source as inverse wave field extrapolation. For a correct extrapolation of the measured wave field, it is required that all sources are positioned on one side of the infinite, continuous measurement plane (i.e. in one half space).

Consider the geometry of Fig 1. Suppose that the pressure *P,* due to a source distribution Ψ in half space *V'* ($y<y_S$), is measured at an infinite, continuous plane *S* (the hologram plane). The position vectors of the measurement positions are indicated with $\mathbf{r}_S$. The pressure *P* at any position $\mathbf{r}_R$ in the complementary half space *V* ($y>y_S$) can be calculated by using the Rayleigh II integral [3] over plane *S*

$$P(\mathbf{r}_R) = \frac{1}{2\pi} \int_{-\infty}^{\infty} \int_{-\infty}^{\infty} P(\mathbf{r}_S) \frac{1 + jk\Delta r}{\Delta r} \cos(\varphi) \frac{e^{-jk\Delta r}}{\Delta r} dx_S\, dz_S \,, \qquad \text{Eq. (2-1)}$$

in which Δr is the distance between a measurement point at position $\mathbf{r}_S$ and the receiver at $\mathbf{r}_R$, while φ is the angle between vector $\mathbf{r}_R$-$\mathbf{r}_S$ and normal **n** at plane *S*. The wave number *k* is given by $2\pi f/c$, in which *f* is the frequency and c the speed of sound.
Using Eq. (2-1), the pressure *P* is extrapolated forward, i.e. to a position further away from the source(s). In order to extrapolate the pressure towards the source(s), the *inverse* operator has to be used, which will not be given here.

2.2 Sampling and truncation of the hologram plane

In practice the hologram cannot be measured at a continuous, infinitely large plane. The data must be spatially sampled and truncated as shown in Fig 2. As a result, the double integral of Eq. (2-1) over the infinite measurement plane *S* can be replaced by a double summation over a finite rectangular grid.
Spatial sampling is allowed if the spatial Nyquist criterion is fulfilled, given by

$$\Delta s < \tfrac{1}{2} \cdot \lambda_{\min} \,, \qquad \text{Eq. (2-2)}$$

in which Δs is the grid spacing and $\lambda_{\min}$ is minimum wave length of interest.
Due to the truncation of the hologram plane *S* the spatial bandwidth is reduced. This means that only for receivers inside the aperture, as seen from the point source Ψ, the pressure *P* can be calculated correctly. This is illustrated in in Fig 2. Note that in the case of multiple sources, the receivers must be inside the aperture of all sources. In order to reduce the diffraction effects due to the truncation, a spatial window or taper must be applied over the hologram.

2.3 '2½D' wave field extrapolation

For the special situation that the sources and the receivers are in the yz-plane, (see Fig 3), it can be shown [4,5] that the double summation over grid *S* can be approximated by a single summation along line *L* (summation over measurement position *m*=1 to M),

$$P(\mathbf{r}_R) = \sqrt{\frac{jk}{2\pi}} \sum_{m=1}^{M} P(\mathbf{r}_m) g(y_{\Psi,L}) \cos(\varphi_m) \frac{e^{-jk\Delta r_m}}{\sqrt{\Delta r_m}} \Delta z \qquad \text{Eq. (2-3)}$$

with amplitude function

$$g(y_{\Psi,L}) = \sqrt{\frac{y_{\Psi,L}}{y_{L,R}}} \; . \qquad \text{Eq. (2-4)}$$

This approximation is valid for $k\Delta r_m >> 1$, i.e. for high frequencies and/or large extrapolation distances. Note that the amplitude function *g* is a function of the distance $y_{\Psi,L}$ between source Ψ and the measurement or hologram line *L*. This means that the source position $\mathbf{r}_\Psi$ (i.e. at least the y-coordinate) must be known a priori.
Eq. (2-3) is also valid when pressure *P* is the result of multiple sources. The only restriction is that all point sources must have the same y-coordinate, i.e. the sources must be positioned along a line parallel to the hologram line.
It can be shown [4] that the '2½D' operator is very similar to the 2D version of the Rayleigh II integral of Eq. (2-1). The only difference is that in the '2½D' case the lateral propagation (i.e. in the x-direction) of the wave field is taken into account, in contrast to the true 2D situation (x-invariant).

It will be clear that the '2½D' wave field extrapolation approach is especially useful for measurements on line arrays in the yz-plane. In contrast to the full 3D operator, which needs 2D input data, the '2½D' operator only requires 1D input data. This significantly reduces measurement time, data storage requirements and computation time.

3 Synthesis of the test array response

Before the experiments took place, the array configuration and its desired response at the boundaries of a fictive hall had to be defined. Starting from this pre-defined array set-up, the optimum driving filters for the array elements are calculated, using the DDS-algorithm. In this section the chosen array configuration and the synthesis (i.e. optimization) procedure will be described.

3.1 Array configuration

The array, which was used during the test, consisted of 6 bass units (Axys Target system, B-215) and 6 top units (Axys Target system, T-2820), as shown in Fig 4. Each bass unit (LxWxH = 1.23x0.55x0.44 m) is equipped with two 15'' woofers. The top units, which have the same dimensions as the bass units, consist of two horn-loaded 1.4'' HF compression drivers and two 10'' MF cone loudspeakers, mounted on a mutual flare. Each woofer pair, MF pair and each individual HF driver can be driven independently. This means that the complete array had 6 LF, 6 MF and 12 HF independent channels with a vertical spacing of 0.44, 0.44 and 0.22 m respectively.
The y-position of the acoustic center of the LF, MF and HF drivers is at 0.08, 0.41 and 0.24 m respectively behind the front of the cabinets.
For each type of driver, a detailed directivity model is available, based on anechoic measured data.

3.2 Optimization geometry

The (fictive) geometry, for which the array was optimized, is shown in Fig 5. The geometry is determined by the floor, rear wall and ceiling. At the symmetry axis of the hall a virtual plane is defined, which is only used for visualization of the synthesized response. It is not taken into account during the optimization.
The bottom of the array was positioned at 2 m above the floor. The audience plane was defined at 1.5 m above the floor.

3.3 Desired SPL distribution

The desired SPL distribution at the boundaries of the hall is shown in Fig 6. The average desired SPL in the audience plane is defined as 100 dB, starting at 103 dB close to the array, decreasing to 97 dB at the rear of the hall. At the ceiling and the rear wall the desired SPL is defined as $-\infty$ dB. Note that SPL values below 80 dB are clipped.

3.4 Optimization of the driving filters

Using the DDS-algorithm, which is based on a 'constrained least squares' optimization scheme, the desired array response is synthesized. Starting from the pre-defined array set-up and the desired SPL distribution, the optimum driving filters are calculated for each channel in the test array.
In practice, these filters are implemented as digital Finite Impulse Response (FIR) filters and delays. The coefficients are uploaded to the DSPs through a network connection between a PC and the Target units.

4 Measurement of the array response

In this section the measurement set-up and method are described.

4.1 Measurement set-up

Since the acoustic centers of the LF, MF and HF drivers are not in the same yz-plane (i.e. at different x-positions), three measurement runs had to be done. As an example, the measurement set-up for the MF drivers in the T-2820 cabinets is shown in Fig 7. For convenience the array was rotated such that its back was on the floor. The measurements were done in a large hall with a height of approx. 8 m. The microphone could be moved along a straight line parallel to the array (i.e in the z-direction). The position of the microphone was measured using a laser distance meter. The distance between the front of the cabinets and the measurement line was defined at 34 mm.
The spatial sampling distance Δz during each of the runs was chosen in relation to the cross-over frequencies of the drivers and the spatial Nyquist criterion of Eq. (2-2):

- LF drivers: Freq. Range = 35 Hz - 150 Hz, $\Delta z = 440$ mm.
- MF drivers: Freq. Range = 150 Hz - 1.4 kHz, $\Delta z = 50$ mm.
- HF drivers: Freq. Range = 1.4 kHz - 18 kHz, $\Delta z = 25$ mm.

Note that the sampling distance for the HF drivers is too large to fulfill the Nyquist criterion for the entire frequency range. The maximum frequency that can be extrapolated correctly is 6.8 kHz. The reason for this is two-fold. First, a smaller sampling distance would result in a too large relative positioning error of the microphone (absolute error was approx. ±2 mm). Secondly, the number of microphone positions would become impractically large for a manually operated positioning system.

4.2 Measurement method

Using a MLSSA-system, impulse responses were taken along the three different measurement lines at the intervals indicated in section 4.1. For the LF, MF and HF measurements, 12, 94 and 190 microphone positions were used respectively.
Since the measurements were done at a short distance from the array, the reflected energy of the ceiling and the side walls of the hall is relatively weak compared to the direct sound. Moreover, these indirect contributions could be removed from the impulse responses by applying a time window of approx. 50 ms.
Note that the floor reflection arrives only a few milliseconds after the direct sound. This means that it can hardly be discriminated from the direct sound, especially at low frequencies. However, due to the large front-to-back ratio of the MF and HF drivers in the cabinets, the reflected energy is relatively low.
For the LF measurements, the floor reflection does play a role. Since the cabinets were put on an acoustically hard floor, the floor reflection will be almost in phase with the direct sound for very low frequencies (35 – 60 Hz). This will result in an increase of pressure. For higher frequencies also destructive interference may occur, depending on the phase relation of the direct and reflected sound.

5 Analysis of the test array response

In this section, both the 'raw' (i.e. unprocessed) measurement data, taken at the hologram line, and the extrapolated results are given. Results are also compared with predictions.

5.1 Measured zt-response

The measured impulse responses are shown in the zt-diagrams of Fig 8 for the LF, MF and HF part of the array respectively. For reasons of visualization, the impulse responses are filtered with a band-limited wavelet. Note that in the MF and HF zt-diagrams, the individual loudspeaker contributions can be clearly identified. Note that z=0 corresponds to the height of the floor in Fig 5.
The initial time-of-flight delay gap is determined by the distance between the acoustic center of the drivers and the measurement line, the DSP filter response time and the MLSSA measurement delay.

5.2 Extrapolated yz-responses

Using the '2½D' operator of Eq. (2-3) and its inverse version, the zt-data of Fig 8 can be extrapolated to other y-positions. In this way a complete set of zt-diagrams can be calculated at different extrapolation distances. By rearranging the obtained yzt-data, a set of yz-diagrams (snapshots) can be obtained at different times. In Fig 9 and Fig 10 several snapshots (yz-diagrams) of the extrapolated array response are shown for the MF and HF part of the array respectively. For positive y-values the pressure is extrapolated forwards, while for negative y-values the data is extrapolated backwards.
Around t=0 ms the individual wave fronts are focused to points. These focus points correspond with the position of the acoustic center of the loudspeakers. Since the upper loudspeakers are 'firing' slightly earlier than the lower ones (see also Fig 8), the lower loudspeakers are not exactly in focus at t=0 ms. Due to the different time delays, the main wave front is slightly tilted downwards, which can be understood by looking at the optimization geometry of Fig 5.

5.3 Far field directivity

In order to calculate the vertical far field polar response of the array, the measured zt-data from each run is extrapolated to a semi-circle with a radius of 1000 m in the yz-plane through the drivers. Next, the extrapolated LF, MF and HF responses are summed. Since the amplitude factor *g* in Eq. (2-3) is a function of the y-position of the acoustic centers, which is different for the LF, MF and HF drivers, the three zt-data sets cannot be summed *before* the extrapolation.
Strictly speaking, the polar responses may not be summed, since the x-offsets of the LF, MF and HF drivers are different. However, at large distances from the array, the x-offsets of the drivers can be ignored, since the horizontal angle between the drivers as seen from the receivers is negligible.
In Fig 11 the measured (i.e. extrapolated) and simulated (i.e. predicted) polar responses are shown for different octave center frequencies. Given the positions of the acoustic centers of the loudspeakers and the length of the hologram line, it can be calculated that the measurement aperture is about 140º (elevation angle -70º to +70º). This means that the measured data is only valid within these limits.
Results show that the measured and simulated far field polar responses agree very well. Especially, the shape of the mean lobe is very well predicted. As expected, at higher angles, near the aperture limits, the differences between the measured and simulated data are larger.

5.4 Frequency response in the audience area

Next, in order to analyze the direct SPL, the measured zt-data is extrapolated to several receiver positions in the (fictive) audience area, (see Fig 5). The receivers are positioned along the center axis of the hall (y-direction) at 5 m intervals, 1.5 m above the floor.
In Fig 12 the measured and simulated 1/3 octave-averaged frequency response are shown. Again, after extrapolation, the LF, MF and HF responses are summed, which is allowed for larger array-to-receiver distances.
Note that the measured and simulated responses correlate very well. The SPL values decrease as a function of distance to the array. It can be verified that the desired SPL, which was defined in section 3.3, is well approximated for the mid and high frequencies. Due to the limited acoustic length of the array for low frequencies, the decrease of SPL as a function of distance is larger in the low-frequency range.
As explained in section 4.2, due to the floor reflection in the measurement set-up, the measured LF SPL is expected to be higher than the predicted SPL. Although, this effect seems to be confirmed by the results, it must be noted that an accurate, quantitative comparison between measured and predicted data at low frequencies is not possible, due to:

- The limited frequency resolution in the measured frequency responses due to the length of the applied time window (50 ms).
- A poor LF signal-to-noise ratio in the measured impulse responses.
- Errors in the extrapolated data since '2½D' conditions are not fulfilled for low frequencies and/or short distances.
- The effect of the increased baffle size on the LF-efficiency and LF-directivity of the loudspeakers.

6 Conclusions

An adapted 'Near field Acoustic Holography' technique was applied to analyse the response of a DDS-driven line array. The advantages of using this method are the following:

- Anechoic measurement conditions are not essential, since measurements can be done at a short distance from the array. As a result, reflected energy is relatively weak compared to the direct sound energy.
- For line array measurements, a '2½D' wave field extrapolation operator can be used, which only needs 1D measurement data. For planar array measurements the full 3D Rayleigh operator must be used, which requires 2D input data.
- Both near field and far field direct sound information can be obtained by extrapolating the measured holographic data.

The disadvantages are:

- For large arrays and/or high frequencies data acquisition is time-consuming. An automatic microphone positioning system is recommended.
- More post-processing is needed compared to traditional straightforward measurements.

From the results it can be concluded that the measured array response is well predicted by the simulations.

7 REFERENCES

1. G.W.J. van Beuningen & E.W. Start.
   Optimizing directivity properties of DSP-controlled loudspeaker arrays.
   Proceedings of the Institute of Acoustics (Reproduced sound) Vol 22 part 6 (2000), p 17 - 37.

2. E.W. Start &. G.W.J. van Beuningen
   Digital Directivity Synthesis of DSP-controlled loudspeaker arrays; A new concept
   Journal of the Dutch Acoustic Society, nr. 153. Nov 2000, p 27 - 36.

3. A.J. Berkhout.
   Applied seismic wave theory
   Elsevier, Amsterdam (1987)

4. E.W. Start.
   Direct sound enhancement by wave field synthesis.
   Ph-D thesis, Delft University of Technology, 1997

5. N. Bleistein.
   Mathematical methods for wave phenomena
   Academic Press Inc., Orlando (1984)

FIGURES

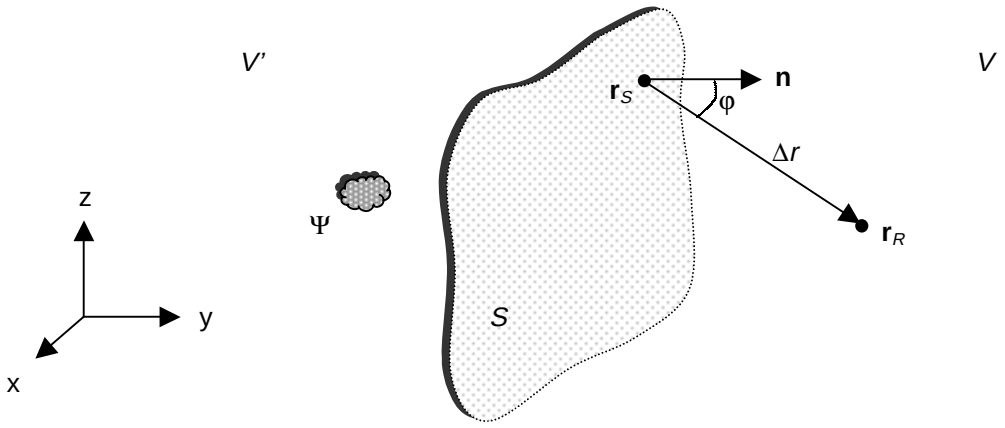

Fig 1 3D Rayleigh II configuration. The pressure *P,* due to source distribution Ψ in half space *V',* is measured at a continuous, infinite plane *S* and is extrapolated to point *R* at position $\mathbf{r}_R$ in half space *V.*

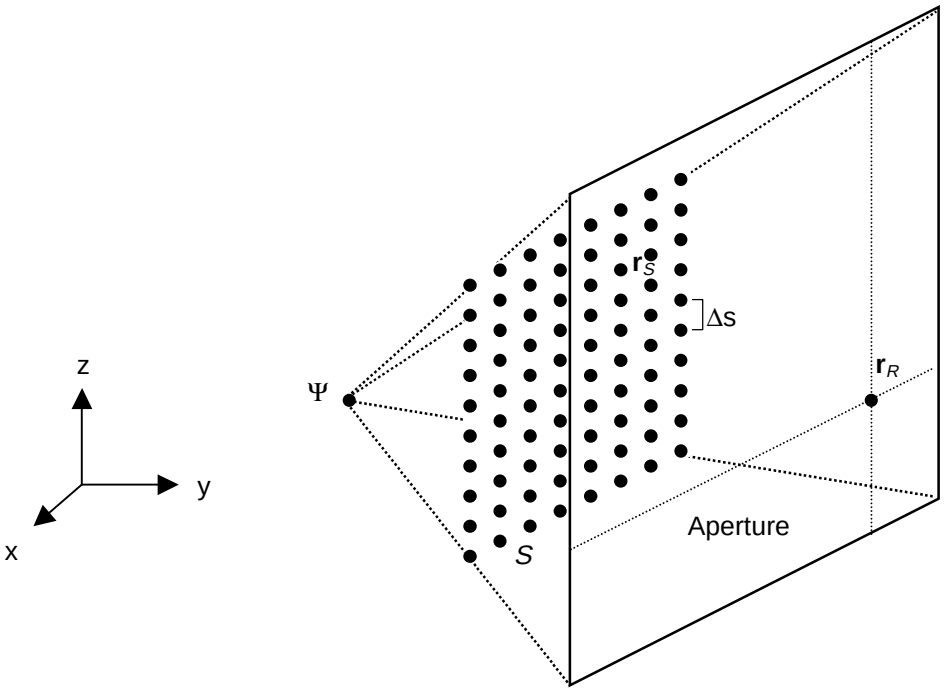

Fig 2 Due to truncation of the hologram plane *S* the extrapolation volume is reduced. The receiver point at position $\mathbf{r}_R$ must be inside the aperture (as seen from the point source Ψ*).*

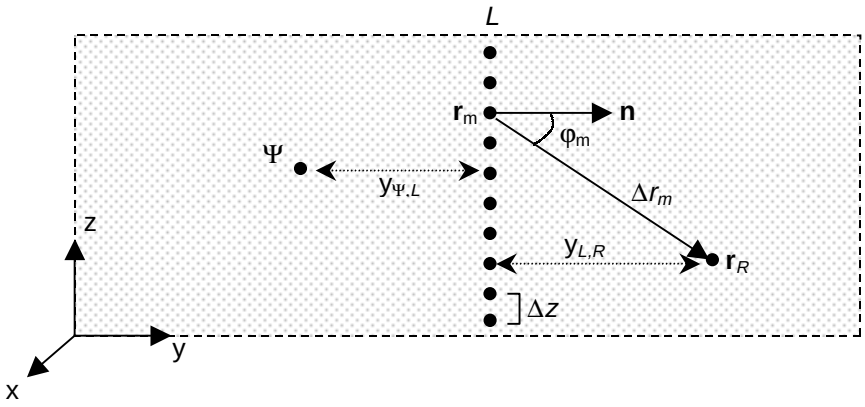

Fig 3 '2½D' configuration. The pressure *P* is measured along line *L* at discrete positions $\mathbf{r}_m$ and is extrapolated to point *R* at position $\mathbf{r}_R$.

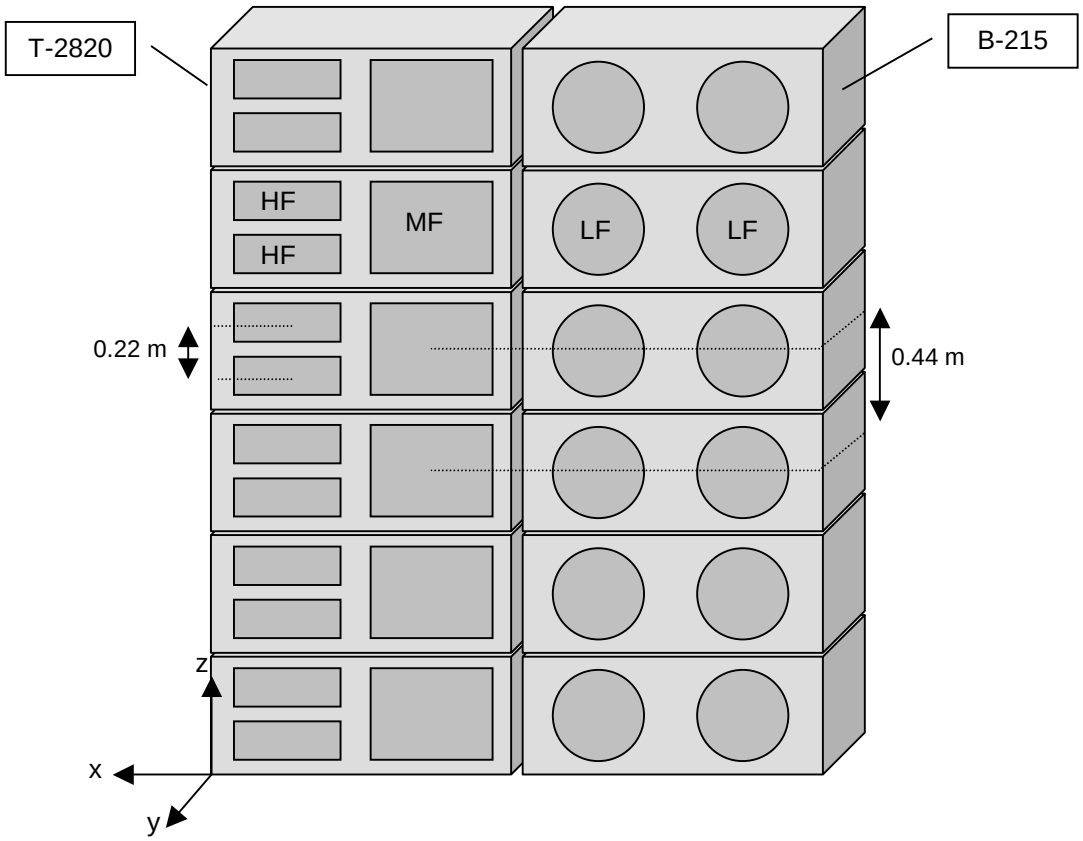

Fig 4 Test array set-up.

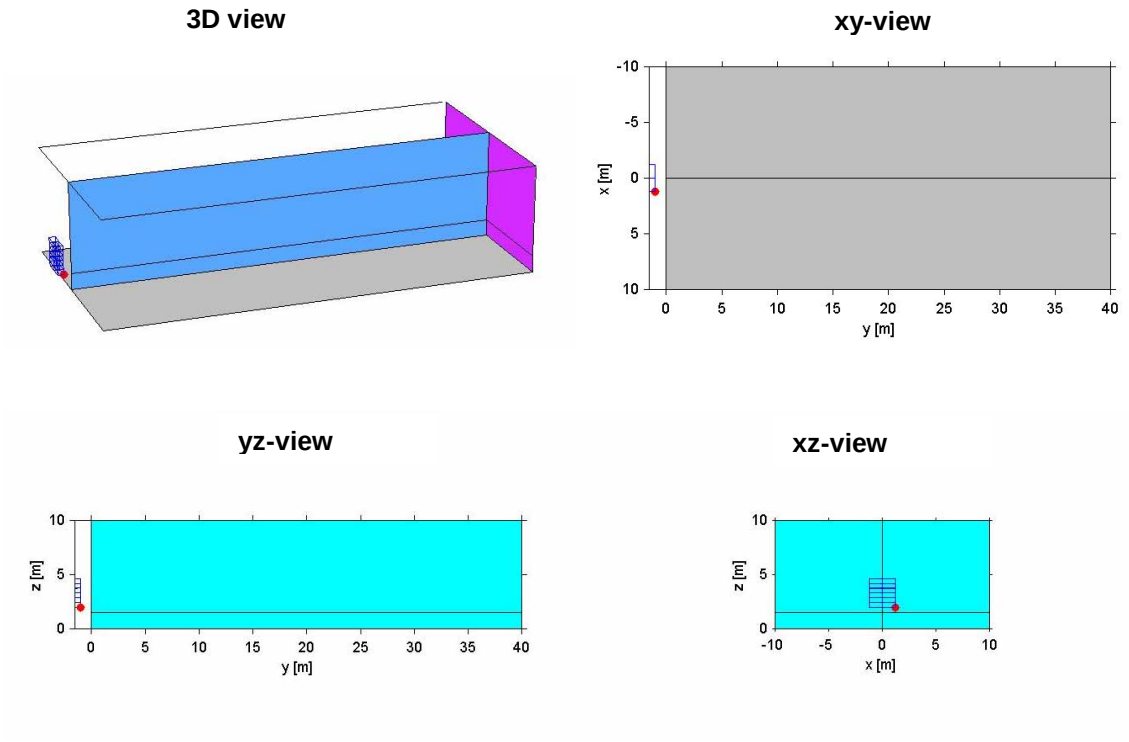

Fig 5 Optimization geometry.

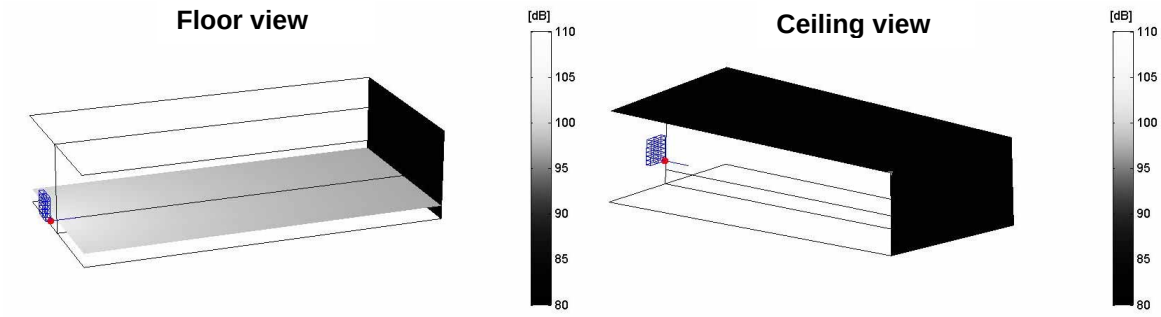

Fig 6 Desired SPL distribution along the boundaries of the hall.

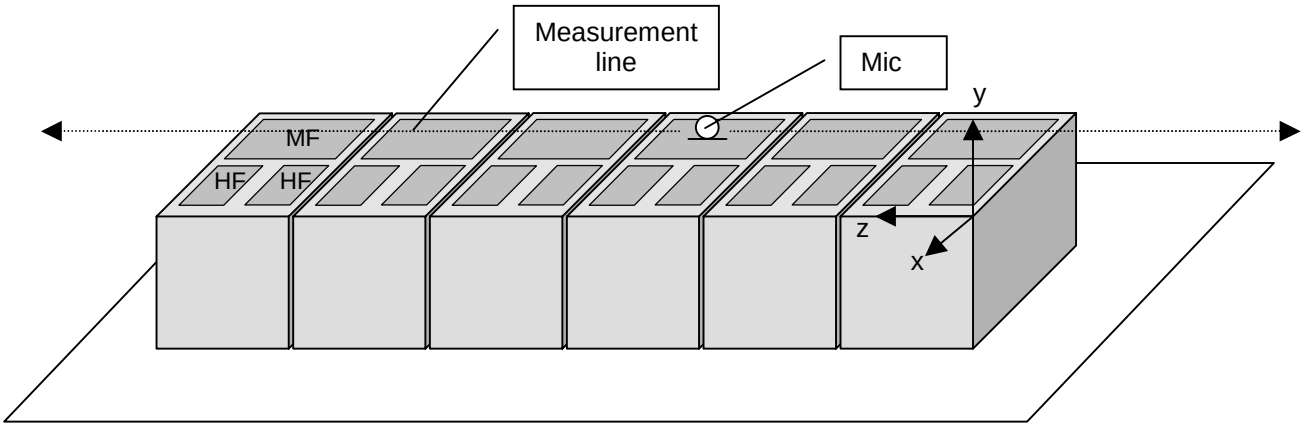

Fig 7 Measurement set-up for the MF drivers. The microphone is moved over the MF part of the array at a distance of 34 mm from the front of the cabinets. The measurement line (length 4.7 m) is sampled at 50 mm intervals.

LF response

MF response

HF response

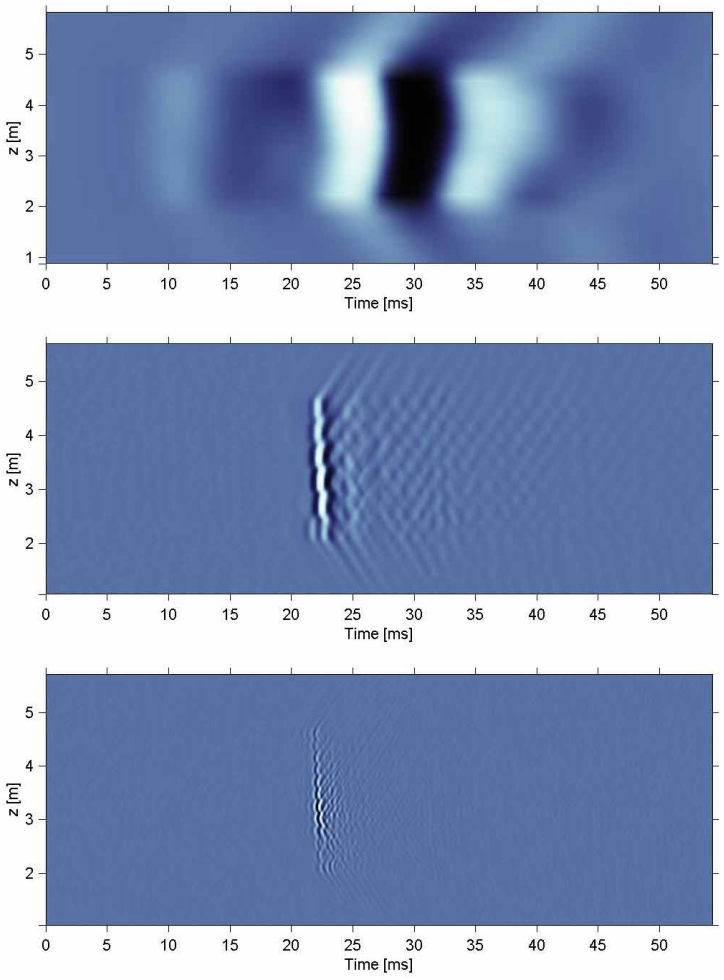

Fig 8 Measured impulse responses along the z-axis for the LF, MF and HF drivers. Note that the bottom of the array is at 2.0 m above the floor, as shown in Fig 5.

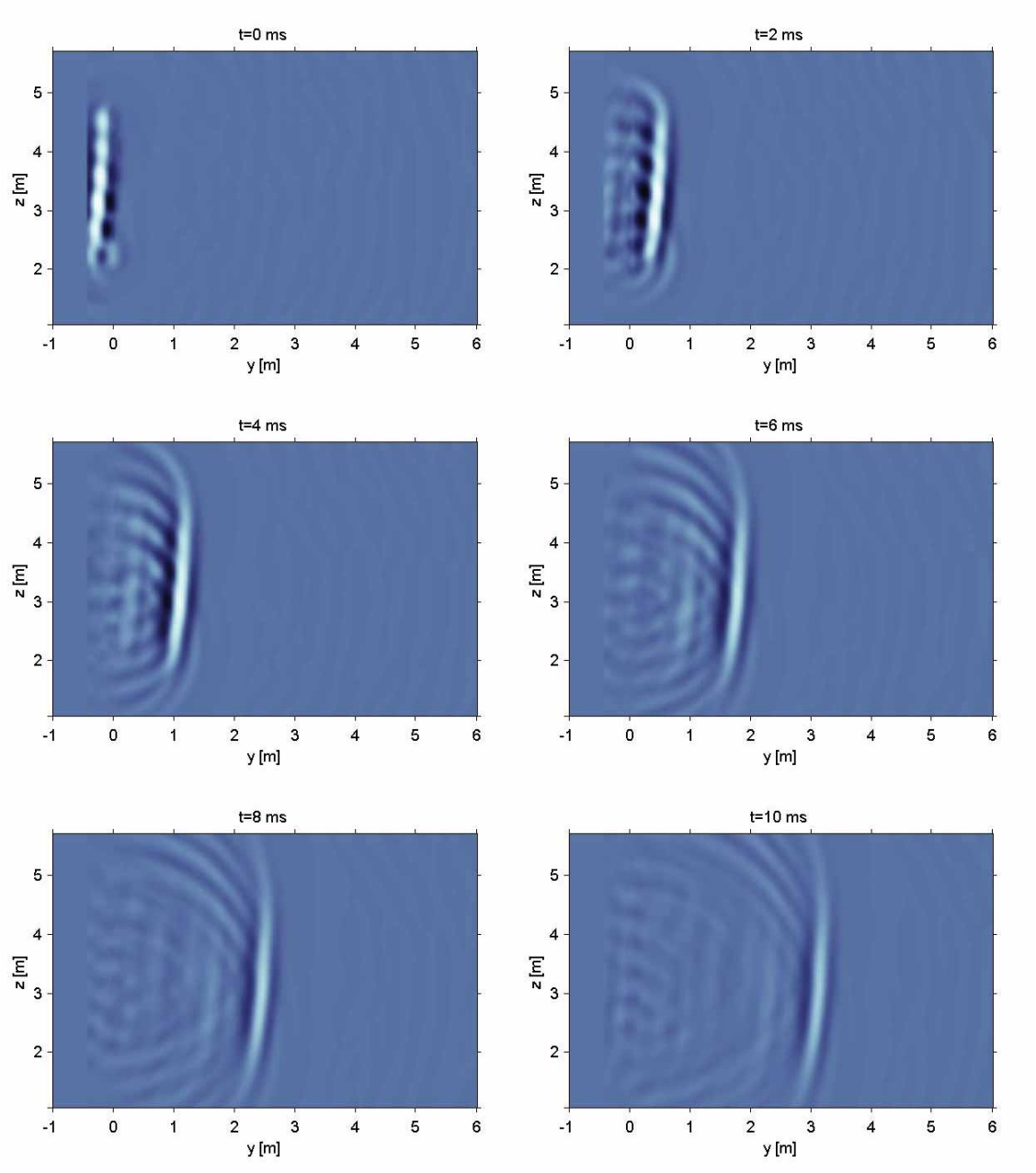

Fig 9 Snapshots (yz-diagrams) of the extrapolated measured zt-data for the MF part of the array. (y is the extrapolation distance).

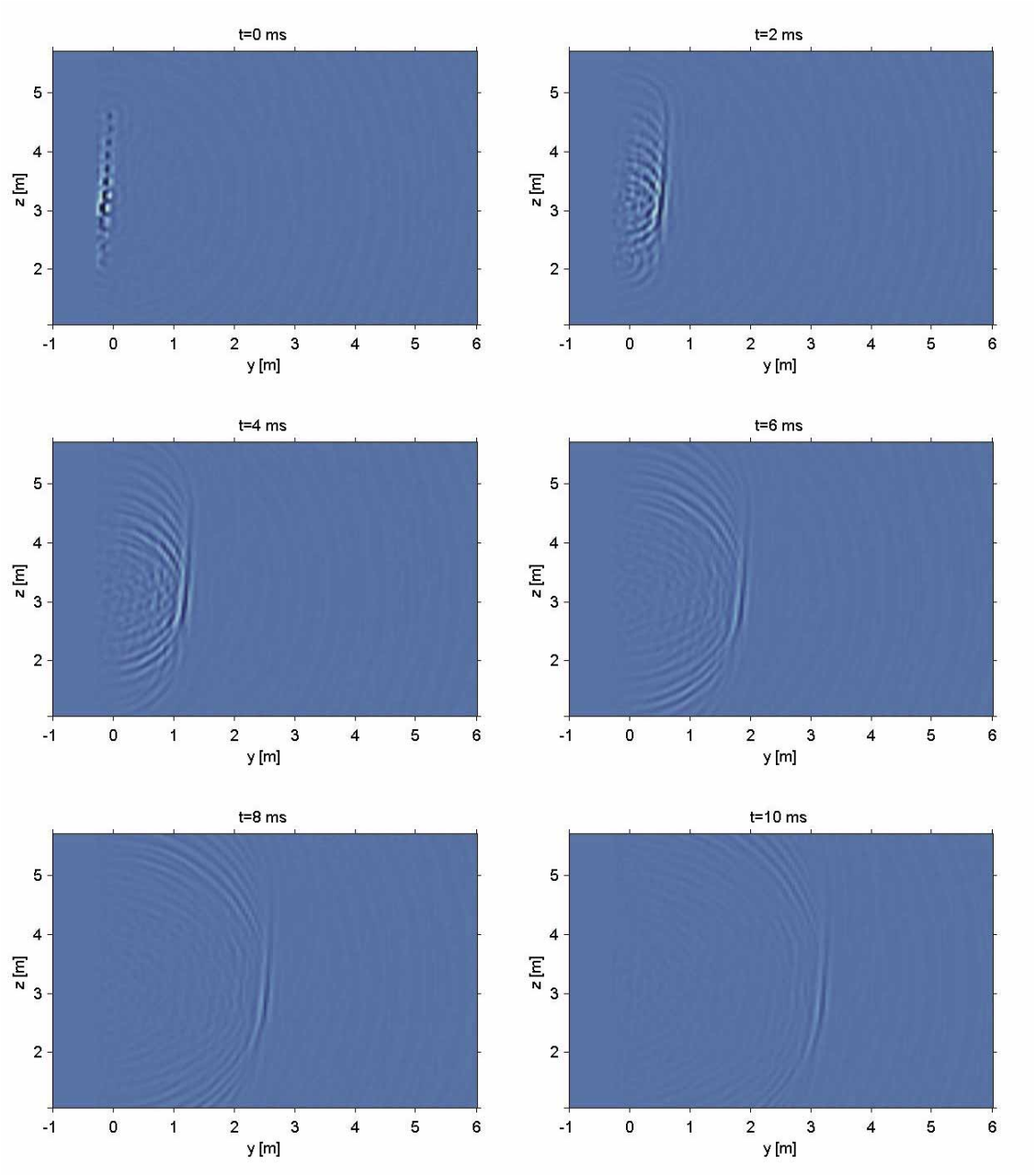

Fig 10 Snapshots (yz-diagrams) of the extrapolated measured zt-data for the HF part of the array. (y is the extrapolation distance).

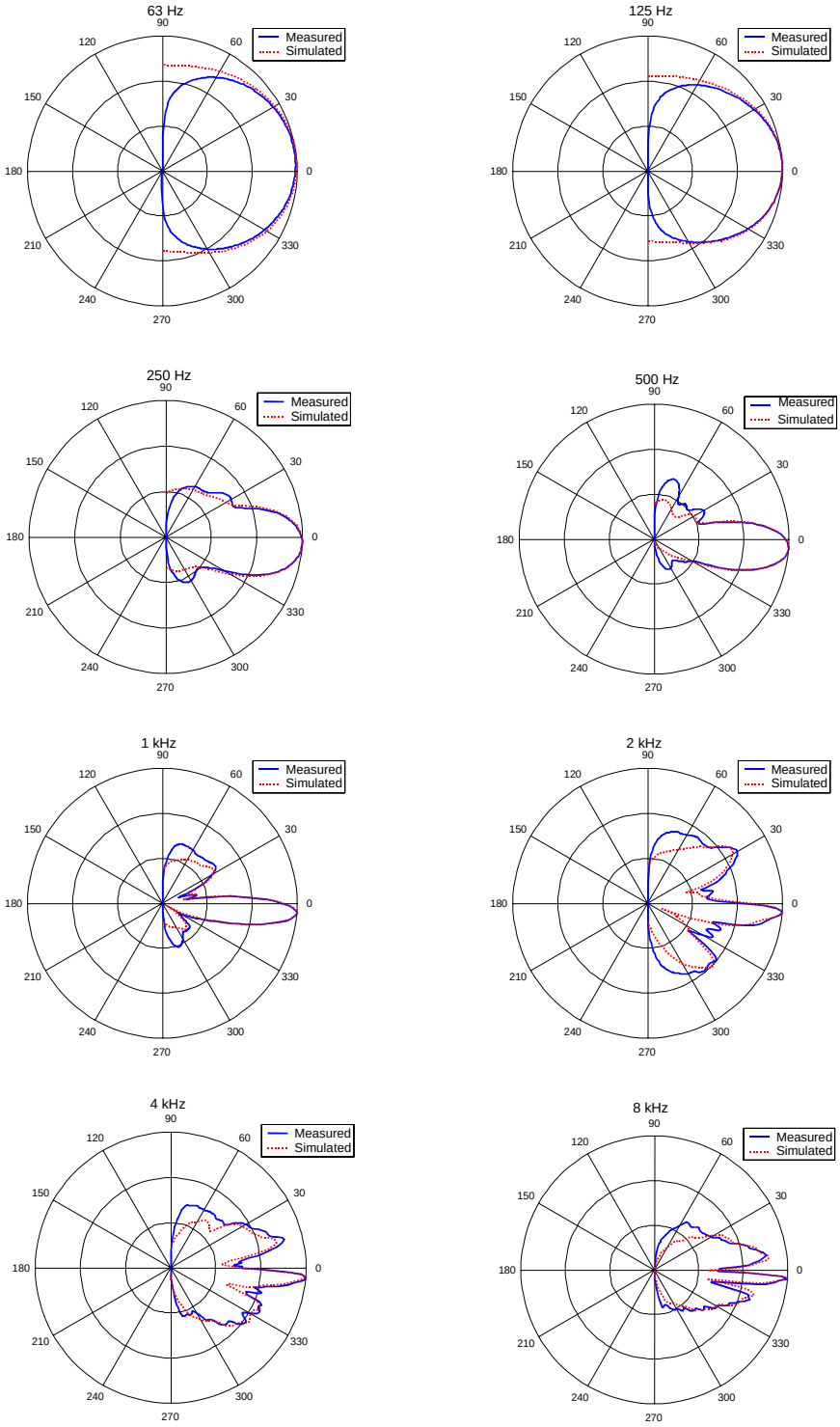

Fig 11 Measured (i.e. extrapolated from measurements) and simulated (i.e. predicted) vertical polar responses of the test array for different octave center frequencies (10 dB/div). Measured values are only valid between –70º and +70º.

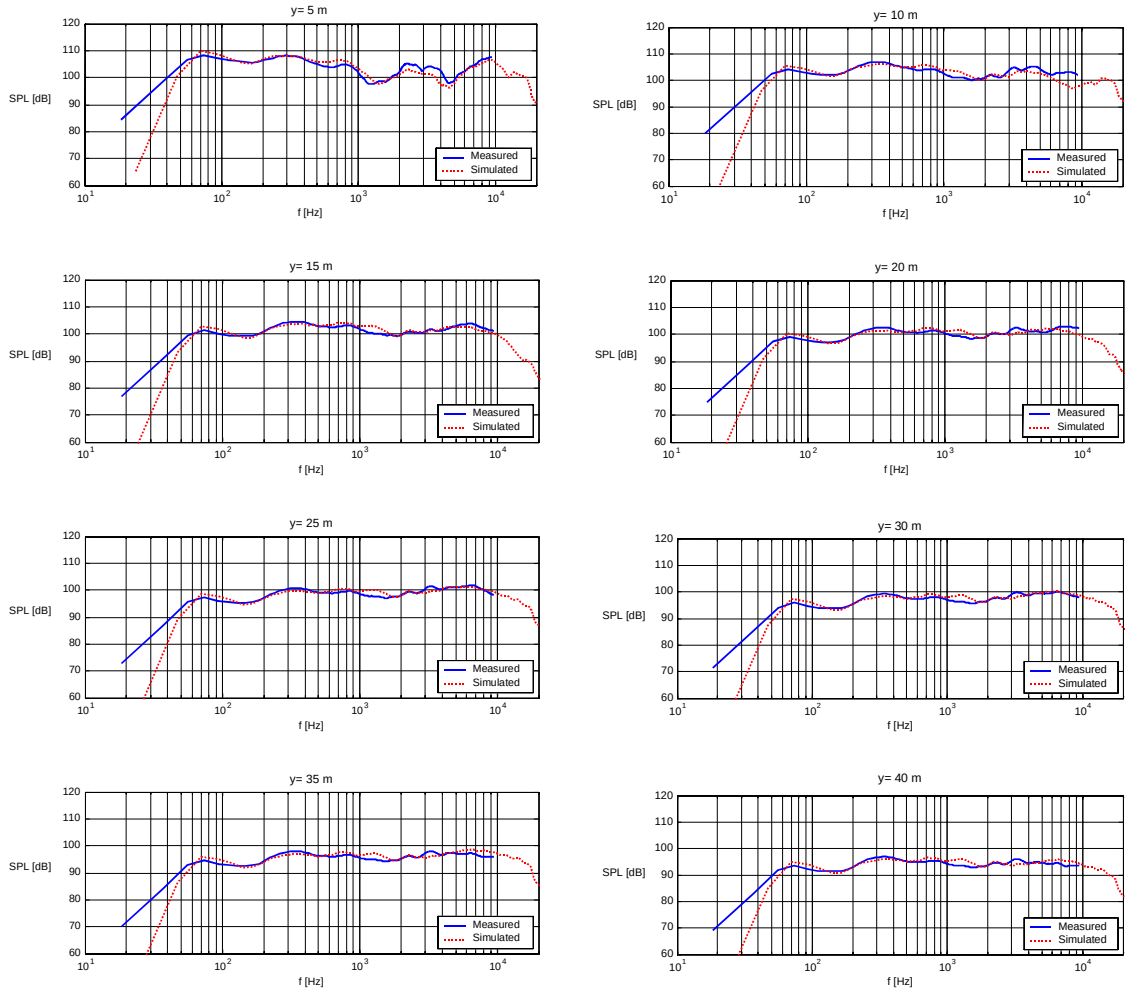

Fig 12 Measured (i.e. extrapolated from measurements) and simulated (i.e. predicted) 1/3 octave averaged frequency responses of the test array at different receiver positions in the fictive hall. Positions are taken along the center axis of the hall (y-direction) at 5 m intervals, 1.5 m above the floor.